# Supplementary Document for RSS 2023 Paper Path Planning for Multiple Tethered Robots Using Topological Braids

## 1 Proof for Lemma 3.5

### 1.1 Main Proof

*Proof.* Given a polygonal trajectory $\xi_i$ with the maximum angle of rotation $\gamma_i$, there exists a range of projection angles $\alpha \in \mathcal{D} = (-\beta, -\beta+\gamma_i) \cup (\pi-\beta, \pi-\beta+\gamma_i)$, such that the projected trajectory $\xi_i^\alpha$ is non-monotonic with respect to $t$ (see Section 1.2 of this supplementary document for the detailed justification for this statement). $\beta \in [-\pi, \pi]$ is an angle specific to each trajectory. Projection angles that fall in different ranges are illustrated by the blue arrows in Figure 1, and illustrations of monotonic and non-monotonic projections are shown in the bottom left and bottom right of Figure 1, respectively. To obtain a non-monotonic projected trajectory, we first construct a set of $2m$ projection angles $\tilde{\mathcal{A}} = \{\frac{i}{m}\pi | i = 0 \dots 2m-1\}$ that uniformly span the range $[0, 2\pi]$. Since $\mathcal{D}$ is the union of two open intervals with an equal length $\gamma_i$, to ensure at least one of the samples falls in one of the intervals, the separation between consecutive samples should be smaller than $\gamma_i$, i.e., $\frac{1}{m}\pi < \gamma_i$. Since $\gamma_i \geq \phi$, a non-monotonic projected trajectory is guaranteed to be obtained by choosing $m > \frac{\pi}{\phi}$. Furthermore, the projections obtained at angles $\frac{i}{m}\pi$ and $\frac{m+i}{m}\pi$, $i = 0 \dots m-1$, are mirror images of each other. Hence, it is sufficient to sample in the range $[0, \pi]$ with $\mathcal{A}(m) = \{\frac{i}{m}\pi | i = 0 \dots m, m \in \mathbb{Z}^+\}$.

Now, consider a set of $\phi$-entangled polygonal trajectories in its fully retracted configuration $\{\xi_i\}_{i \in \mathcal{I}_n}$, i.e., $\gamma(\{\xi_i\}_{i \in \mathcal{I}_n}) = \underline{\gamma} = \phi$. Let $\xi_i$ be the trajectory that has $\gamma_i = \underline{\gamma}$. From the previous paragraph, we know that the non-monotonic projection of $\xi_i$ is guaranteed to be obtained at a projection angle $\alpha_0 \in \mathcal{A}(m)$ for $m > \frac{\pi}{\phi}$. The projected trajectory $\xi_i^{\alpha_0}$ bounds a polygon area, as shown by the light blue region in the bottom left of Figure 1. At least

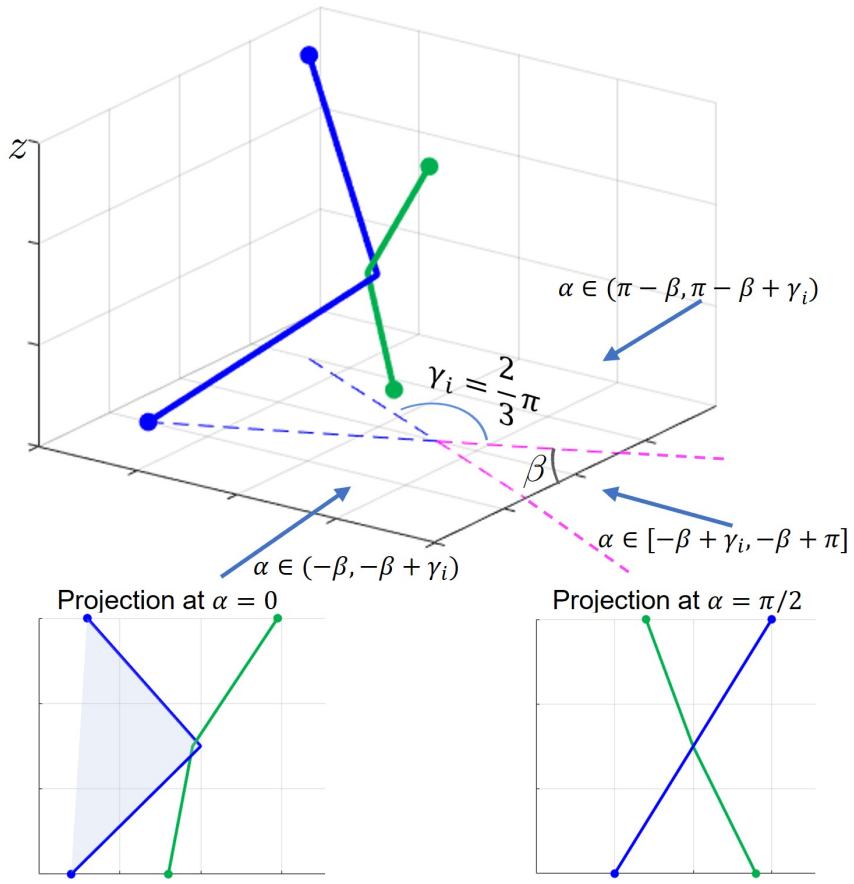


Figure 1: An illustration of entanglement. The blue and green solid lines are the cables/trajectories of robot $i$ and $j$. The blue dashed lines are the cable/trajectory of robot $i$ projected onto the X-Y plane. The bottom two plots show the projections of the cables/trajectories onto a plane $\mathcal{P}(\alpha)$. In the bottom left plot, the blue projected trajectory is non-monotonic.

one of the other trajectories intersects the polygon (e.g., the green trajectory in Figure 1); otherwise, $\xi_i$ can be further straightened and $\gamma_i$ can be further reduced while keeping $\gamma_j$ constant for all $j \in \mathcal{I}_n \backslash i$, resulting in $\gamma < \underline{\gamma}$, a contradiction. On the projection plane $\mathcal{P}(\alpha_0)$, any attempt to further straighten $\xi_i^{\alpha_0}$ always results in an increase in the bending of the other trajectories, and it is impossible to straighten all trajectories without allowing them to penetrate each other. Hence, $\{\xi_i^{\alpha_0}\}_{i \in \mathcal{I}_n}$ is non-isotopic to a set of straight lines. Furthermore, any isotopic trajectories have isotopic projections under the same projection angle, because every elementary move in 3-D can be projected to a move in 2-D that also preserves isotopy. As a result, for all space-time trajectories isotopic to $\{\xi_i\}_{i \in \mathcal{I}_n}$, there exists an angle $\alpha_0 \in \mathcal{A}(m)$, such that the projected trajectories are non-isotopic to a set of straight lines. $\square$

## 1.2 Justification of Statement

Given a polygonal trajectory $\xi_i$ with the maximum angle of rotation $\gamma_i$, there exists a range of projection angles $\alpha \in \mathcal{D} = (-\beta, -\beta+\gamma_i) \cup (\pi-\beta, \pi-\beta+\gamma_i)$, such that the projection of $\xi_i$ onto $\mathcal{P}(\alpha)$, denoted as $\xi_i^{\alpha}$, is non-monotonic with respect to $t$.

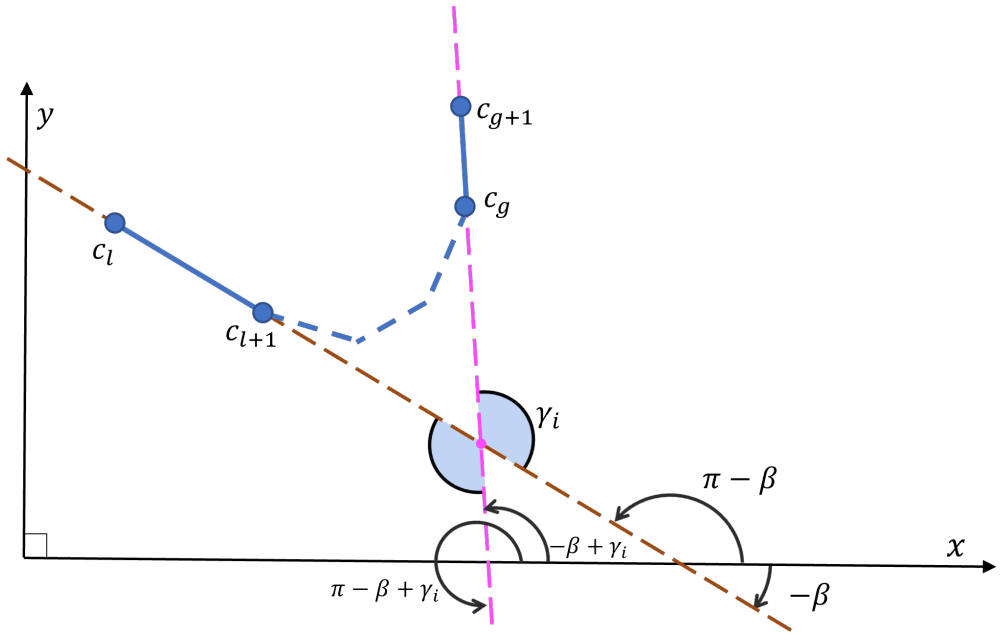


Figure 2: $\xi_i$ projected onto the X-Y plane.

To justify the above statement, consider a polygonal trajectory $\xi_i$ with the maximum angle of rotation $\gamma_i$. The projection of $\xi_i$ onto the X-Y plane is shown in Figure 2 above, where the maximum angle of rotation occurs between the projected segments $\overline{c_l c_{l+1}}$ and $\overline{c_g c_{g+1}}$ (the solid blue segments), and the dashed blue lines indicate arbitrary projected segments between $c_{l+1}$ and $c_g$. $\beta$ is the acute angle between the $x$-axis and the extension line of $\overline{c_l c_{l+1}}$ (the brown line). Consider a line $\mathcal{L}(\alpha)$ obtained by rotating the $x$-axis by an angle $\alpha$. In Figure 2, the brown line is parallel to $\mathcal{L}(-\beta)$ and $\mathcal{L}(\pi-\beta)$, while the pink line is parallel to $\mathcal{L}(-\beta+\gamma_i)$ and $\mathcal{L}(\pi-\beta+\gamma_i)$. For each $\alpha \in \mathcal{D} = [-\beta, -\beta+\gamma_i] \cup [\pi-\beta, \pi-\beta+\gamma_i]$, there always exists a line parallel to $\mathcal{L}(\alpha)$ that cuts the segments $\overline{c_l c_{l+1} \ldots c_g c_{g+1}}$ more than once, regardless of the shape of the segments between $c_{l+1}$ and $c_g$. To see this, consider a line $\tilde{\mathcal{L}}$ passing through the intersection between the brown line and the pink line (the pink point), and passing through the interiors of two light blue-shaded arcs. In this way, $\tilde{\mathcal{L}}$ is parallel to $\mathcal{L}(\alpha)$ for an $\alpha \in \mathcal{D}$. If we shift $\tilde{\mathcal{L}}$ vertically upwards (i.e., increasing the $y$-coordinate of $\tilde{\mathcal{L}}$ at every $x$) while keeping its gradient, we can move $\tilde{\mathcal{L}}$ until it intersects with $\overline{c_l c_{l+1} \ldots c_g c_{g+1}}$ more than once.

In 3-D, this means that there always exists a plane perpendicular to both the X-Y plane and $\mathcal{P}(\alpha)$, that intersects $\xi_i$ more than once. Furthermore, since $\xi_i$ is ascending in $t$, the intersections occur at different $t$. As a result, when $\xi_i$ is projected onto the plane $\mathcal{P}(\alpha)$, there always exists a vertical line that intersects the projected trajectory $\xi_i^\alpha$ more than once. Hence, $\xi_i^\alpha$ is non-monotonic for $\alpha \in \mathcal{D}$.

# 2 Supplementary proof for Lemma 3.6

Given a non-straight polygonal trajectory, the polygon bounded by the trajectory can be partitioned into multiple triangles. There always exist a set of triangles and a sequence of evaluating the triangles for the application of elementary moves, that satisfy the following conditions:

(1) the triangles can be classified into the four types defined in Figure 7 in the paper;

(2) the evaluation of triangles follows a temporal sequence;

(3) both the edges before and after an elementary move should be ascending.

To justify the above statement, consider a non-straight polygonal projected trajectory $\xi_i^\alpha$, which bounds a polygon region that contains the projections of other trajectories. Figure 3(a) in this document shows an example, where two projected trajectories $\xi_j^\alpha$ and $\xi_k^\alpha$ pass the interior of the polygon bounded by $\xi_i^\alpha$ (the blue line segments). Suppose we would like to obtain a sequence of elementary moves that transform $\xi_i^\alpha$ into a straight line (the dashed line segment). We can construct two chains of triangles that fully contain $\xi_j^\alpha$ and $\xi_k^\alpha$, as shown in Figure 3(a). A type I triangle is at the intersection between trajectories $j$ and $k$, while all other triangles are of type II or III. The intersections between $\xi_i^\alpha$ and the other two trajectories separate $\xi_i^\alpha$ into three parts; we pick the part bounded by two intersection points and transform it, using a sequence of elementary moves, to the boundary of the chain containing the lower section of $\xi_k^\alpha$ and the upper section of $\xi_j^\alpha$ (the dash-dotted blue line in Figure 3(b)). This transformation can be done because the area bounded by the initial and the transformed trajectories is empty and can be partitioned into triangles of type IV. Furthermore, both the initial and the transformed trajectories are ascending. Then, the chain of triangles containing trajectory $k$ can be evaluated following a permissible sequence indicated by the numbering in Figure 3(b). If elementary moves can be applied to all these triangles, trajectory $i$ can be further transformed to the configuration shown in Figure 3(c). Notice that in triangle 15, trajectory $j$ crosses trajectory $k$. Hence, in order to evaluate triangle 15, the temporal sequence requires the lower section of trajectory $j$ to be evaluated

first. To do so, the lower part of trajectory $i$ is further transformed to the boundary of the chain containing the trajectory $j$ (Figure 3(d)). This is possible because the blue region in Figure 3(c) is empty. Then, the sequence of triangles 10 to 18 can be evaluated and results in a transformed trajectory in Figure 3(e) if elementary moves are successfully applied to all triangles. To finish the transformation, the following steps can be followed. First, transform the upper section of trajectory $i$ to the boundary of trajectory $j$ by applying elementary moves to the orange region in Figure 3(e). Second, apply a sequence of evaluations to the chain of triangles 19 to 25. Finally, transform trajectory $i$ across the empty space illustrated by the green region. Note that the temporal sequence of evaluation is respected throughout the transformation process; furthermore, the transformed trajectory in every step is ascending.

From the above example, we can obtain a general treatment for a non-straight projected trajectory $i$. First, construct a chain of triangles for each of the trajectories in the interior of the polygon bounded by trajectory $i$; the triangles are of type I, II, or III. Pick a section of the trajectory $i$ and transform it across the empty space, until the transformed trajectory becomes the boundary of a chain. Evaluate the triangles in the chain from the bottom to the top, until a triangle is encountered that contains a crossing between two trajectories. For the lower part of trajectory $i$ that has been transformed across the chain, continue to transform it across the empty space, until reaching the boundary of another chain. Evaluate the triangles in the chain from the bottom to the top, until meeting a triangle that contains a crossing point. Check whether the lower sections of the two crossing trajectories have been evaluated; if yes, the triangle containing the crossing point can be evaluated; if not, continue to transform the lower part of the trajectory $i$ until meeting the boundary of another chain, and evaluate the chain of triangles. This procedure can be conducted iteratively until trajectory $i$ is successfully transformed into a straight line, or a triangle is encountered to which the elementary move cannot be applied (a tangle).

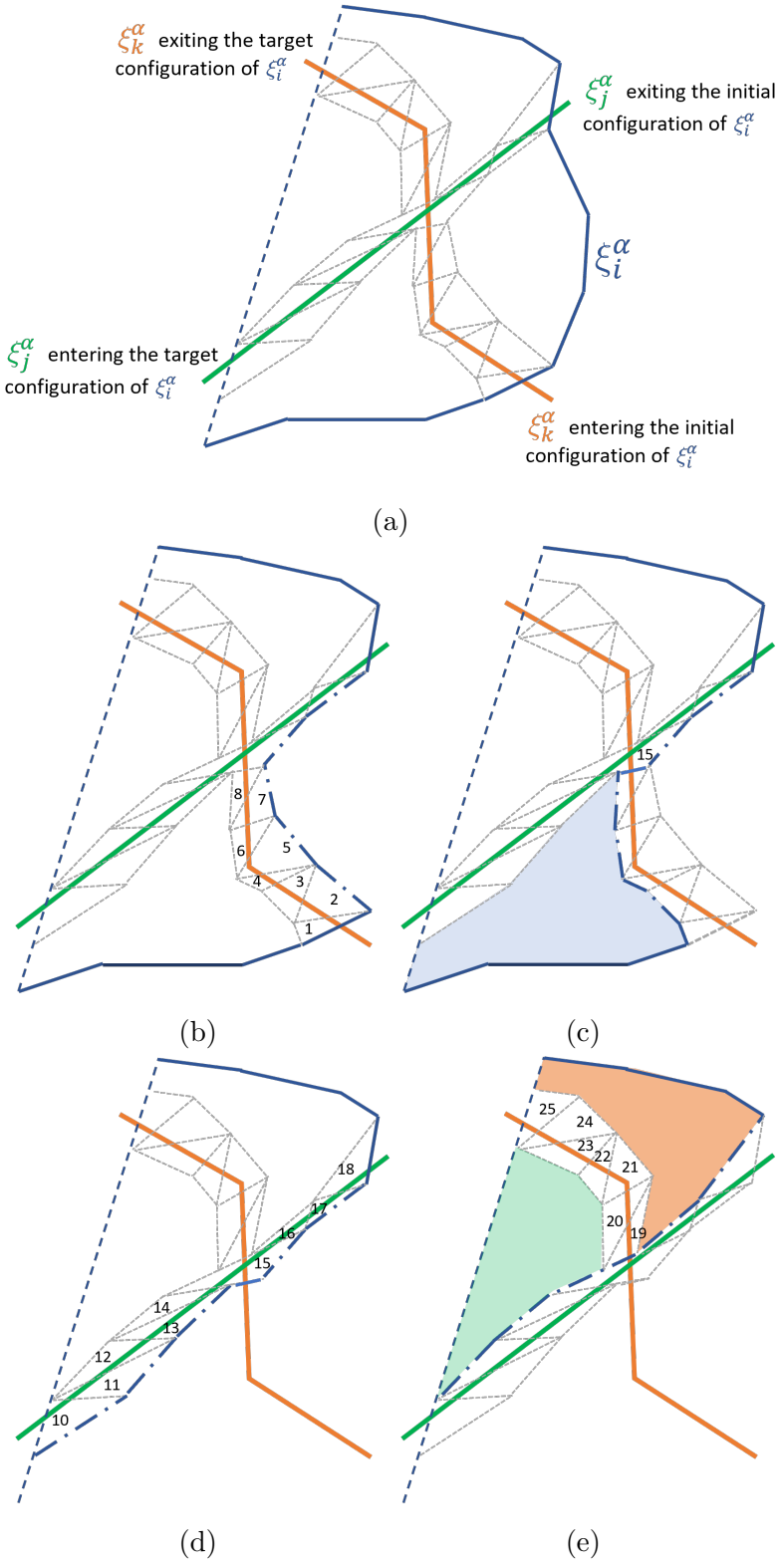


Figure 3: A sequence of transformations of trajectory $i$.

# 3 Pseudocodes for Algorithms

**Algorithm 1:** Update and check 2-braid

**Input:** $b^l_{i,j}$, $\tau$

**Output:** $b^l_{i,j}$,valid

```
function updateCheck2Braid
    valid = true
    if b^l_{i,j} == e then
        b^l_{i,j} = τ
    else if b^l_{i,j} == τ then
        valid = false
    else
        b^l_{i,j} = e
    return [b^l_{i,j}, valid];
```

**Algorithm 2:** Update and check 3-braid

**Input:** $b^l_{i,j,k}$, $\tau$

**Output:** $b^l_{i,j,k}$,valid

**function** updateCheck3Braid
    valid = true
    **if** *lastElement*($b^l_{i,j,k}$)== $-\tau$ **then**
        remove the last element of $b^l_{i,j,k}$
    **else**
        Append $\tau$ to $b^l_{i,j,k}$
    **if** *length*($b^l_{i,j,k}$)== 3 **then**
        **if** $b^l_{i,j,k} \in \{\sigma_f^c \sigma_g^{-c} \sigma_f^c | c \in \{1,-1\}, f,g \in \{1,2\}, f \neq g\}$ **then**
            valid = false
    **else if** *length*($b^l_{i,j,k}$)== 4 **then**
        reduce $b^l_{i,j,k}$ based on pre-computed actions (See Table 1)
    return [$b^l_{i,j,k}$, valid];

Table 1: Precomputed list of possible 3-braids with length 3 and 4

| Length 3 | subsequent braids with length 4 | actions |
|---|---|---|
| $\sigma_1\sigma_2\sigma_1$ | $\sigma_1\sigma_2\sigma_1\sigma_2$ | rejected because equivalent to $\sigma_2\sigma_1\sigma_2\sigma_2$ |
| | $\sigma_1\sigma_2\sigma_1\sigma_2^{-1}$ | reduced to $\sigma_2\sigma_1$ |
| $\sigma_1\sigma_2\sigma_1^{-1}$ | $\sigma_1\sigma_2\sigma_1^{-1}\sigma_2$ | rejected because equivalent to $\sigma_2^{-1}\sigma_1\sigma_2\sigma_2$ |
| | $\sigma_1\sigma_2\sigma_1^{-1}\sigma_2^{-1}$ | reduced to $\sigma_2^{-1}\sigma_1$ |
| $\sigma_1\sigma_2^{-1}\sigma_1$ | | equivalent to a 3-braid tangle, rejected |
| $\sigma_1\sigma_2^{-1}\sigma_1^{-1}$ | $\sigma_1\sigma_2^{-1}\sigma_1^{-1}\sigma_2$ | rejected because equivalent to $\sigma_2^{-1}\sigma_1^{-1}\sigma_2\sigma_2$ |
| | $\sigma_1\sigma_2^{-1}\sigma_1^{-1}\sigma_2^{-1}$ | reduced to $\sigma_2^{-1}\sigma_1^{-1}$ |
| $\sigma_1^{-1}\sigma_2^{-1}\sigma_1$ | $\sigma_1^{-1}\sigma_2^{-1}\sigma_1\sigma_2$ | reduced to $\sigma_2\sigma_1^{-1}$ |
| | $\sigma_1^{-1}\sigma_2^{-1}\sigma_1\sigma_2^{-1}$ | rejected because equivalent to $\sigma_2\sigma_1^{-1}\sigma_2^{-1}\sigma_2^{-1}$ |
| $\sigma_1^{-1}\sigma_2^{-1}\sigma_1^{-1}$ | $\sigma_1^{-1}\sigma_2^{-1}\sigma_1^{-1}\sigma_2$ | reduced to $\sigma_2^{-1}\sigma_1^{-1}$ |
| | $\sigma_1^{-1}\sigma_2^{-1}\sigma_1^{-1}\sigma_2^{-1}$ | rejected because equivalent to $\sigma_2^{-1}\sigma_1^{-1}\sigma_2^{-1}\sigma_2^{-1}$ |
| $\sigma_1^{-1}\sigma_2\sigma_1$ | $\sigma_1^{-1}\sigma_2\sigma_1\sigma_2$ | reduced to $\sigma_2\sigma_1$ |
| | $\sigma_1^{-1}\sigma_2\sigma_1\sigma_2^{-1}$ | rejected because equivalent to $\sigma_2\sigma_1\sigma_2^{-1}\sigma_2^{-1}$ |
| $\sigma_1^{-1}\sigma_2\sigma_1^{-1}$ | | equivalent to a 3-braid tangle, rejected |
| $\sigma_2\sigma_1\sigma_2$ | $\sigma_2\sigma_1\sigma_2\sigma_1$ | rejected because equivalent to $\sigma_1\sigma_2\sigma_1\sigma_1$ |
| | $\sigma_2\sigma_1\sigma_2\sigma_1^{-1}$ | reduced to $\sigma_1\sigma_2$ |
| $\sigma_2\sigma_1\sigma_2^{-1}$ | $\sigma_2\sigma_1\sigma_2^{-1}\sigma_1$ | rejected because equivalent to $\sigma_1^{-1}\sigma_2\sigma_1\sigma_1$ |
| | $\sigma_2\sigma_1\sigma_2^{-1}\sigma_1^{-1}$ | reduced to $\sigma_1^{-1}\sigma_2$ |
| $\sigma_2\sigma_1^{-1}\sigma_2$ | | equivalent to a 3-braid tangle, rejected |
| $\sigma_2\sigma_1^{-1}\sigma_2^{-1}$ | $\sigma_2\sigma_1^{-1}\sigma_2^{-1}\sigma_1$ | rejected because equivalent to $\sigma_1^{-1}\sigma_2^{-1}\sigma_1\sigma_1$ |
| | $\sigma_2\sigma_1^{-1}\sigma_2^{-1}\sigma_1^{-1}$ | reduced to $\sigma_1^{-1}\sigma_2^{-1}$ |
| $\sigma_2^{-1}\sigma_1^{-1}\sigma_2$ | $\sigma_2^{-1}\sigma_1^{-1}\sigma_2\sigma_1$ | reduced to $\sigma_1\sigma_2^{-1}$ |
| | $\sigma_2^{-1}\sigma_1^{-1}\sigma_2\sigma_1^{-1}$ | rejected because equivalent to $\sigma_1\sigma_2^{-1}\sigma_1^{-1}\sigma_1^{-1}$ |
| $\sigma_2^{-1}\sigma_1^{-1}\sigma_2^{-1}$ | $\sigma_2^{-1}\sigma_1^{-1}\sigma_2^{-1}\sigma_1$ | reduced to $\sigma_1^{-1}\sigma_2^{-1}$ |
| | $\sigma_2^{-1}\sigma_1^{-1}\sigma_2^{-1}\sigma_1^{-1}$ | rejected because equivalent to $\sigma_1^{-1}\sigma_2^{-1}\sigma_1^{-1}\sigma_1^{-1}$ |
| $\sigma_2^{-1}\sigma_1\sigma_2$ | $\sigma_2^{-1}\sigma_1\sigma_2\sigma_1$ | reduced to $\sigma_1\sigma_2$ |
| | $\sigma_2^{-1}\sigma_1\sigma_2\sigma_1^{-1}$ | rejected because equivalent to $\sigma_1\sigma_2\sigma_1^{-1}\sigma_1^{-1}$ |
| $\sigma_2^{-1}\sigma_1\sigma_2^{-1}$ | | equivalent to a 3-braid tangle, rejected |